Mass Estimation of Merging Galaxy Clusters

(Takizawa, Nagino, & Matsushita 2010: PASJ, 62, 951)

M. Takizawa[1], R. Nagino[2], K. Matsushita[2]
[1] *Yamagata University*
[2] *Tokyo University of Science*

The Fourth East Asia Numerical Astrophysics Meeting
@ASIAA, Taiwan (2010/11/02)

Introduction（1）

- Mass is one of the most fundamental parameters to characterize astrophysical objects. This is especially true in many kinds of self-gravitating objects.
- Mass distribution in large scales such as clusters of galaxies
  - Dark matter properties (self-interaction, MOND, etc)
  - Probes of structure formation
- However, It is not so easy to determine mass in an observational way.
- Cross-checks among different methods are important.
  - line-of-sight velocity distribution of member galaxies + Virial theorem or Jeans equation
  - X-ray observations (n_e, kT) + hydrostatic equilibrium
  - (strong and weak) gravitational lensing

Introduction（2）

However, inconsistent results are sometimes obtained from different methods for a single object.

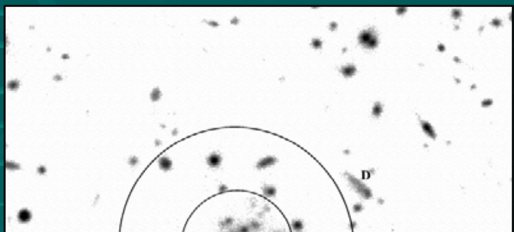

•CL 0024+17 (Ota et al. 2004, Broadhurst et al. 2000, Jee et al. 2007, Umetsu et al. 2010,,,,)
Sugnificant mass discrepancy within 200 kpc.

$M_{Lens}/M_X \sim 2\text{--}3$

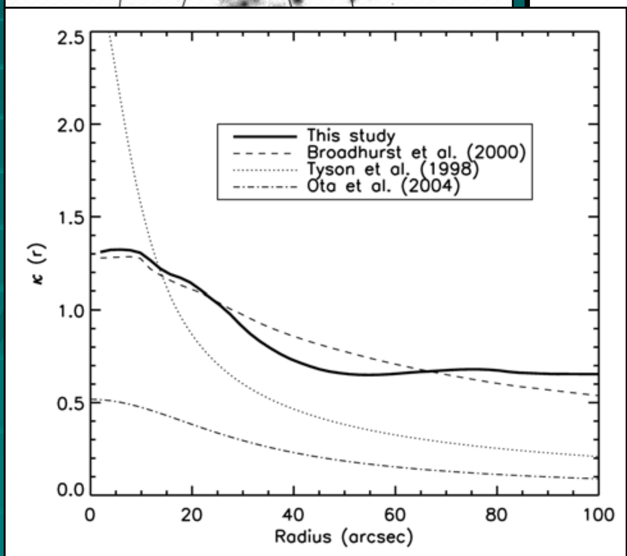

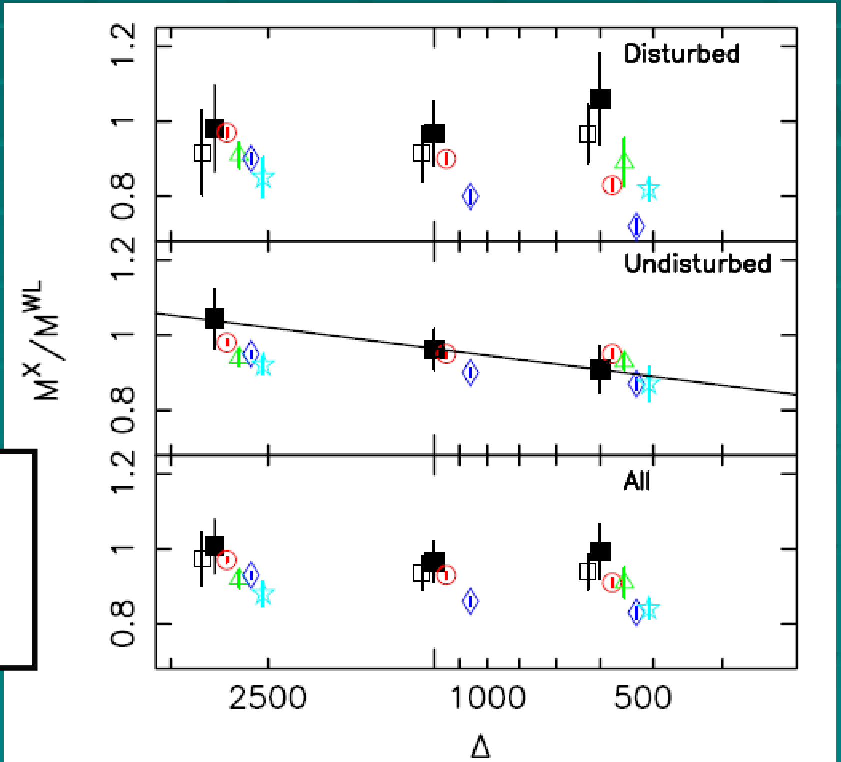

•“Disturbed Clusters” tend to show larger mass discrepancy （Zhang et al. 2010）.

Introduction(3)

- Some assumptions are necessary in mass estimation.
  - M_X (hydrostatic equilibrium, spherical symmetry）
  - M_{lens} (geometry)
  - M_{virial} (dynamical equilibrium、isotropic velocity dispersion ,etc）
- These assumptions are not very good in clusters during or a few Gyr after mergers.
- It is not trivial how these systems will be overestimated or underestimated.
- Using N-body + hydrodynamical simulation data, “simulations of mass estimation” are performed, and the results are compared with “real mass distribution” in the data.

Simulation Data（N-body＋hydrodynamics）

Mass distribution

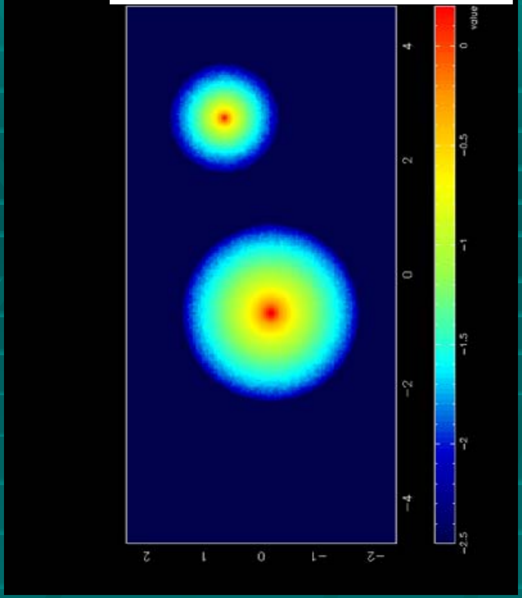

- N-body：Particle Mesh (PM) method
- self-gravity：FFT with isolated boundary conditions
- hydrodynamics：Roe TVD method
- number of grid points $256 \times 128 \times 128$
- Number of particles $256 \times 128 \times 128$ ($\fallingdotseq 4.2 \times 10^6$)

Gas density

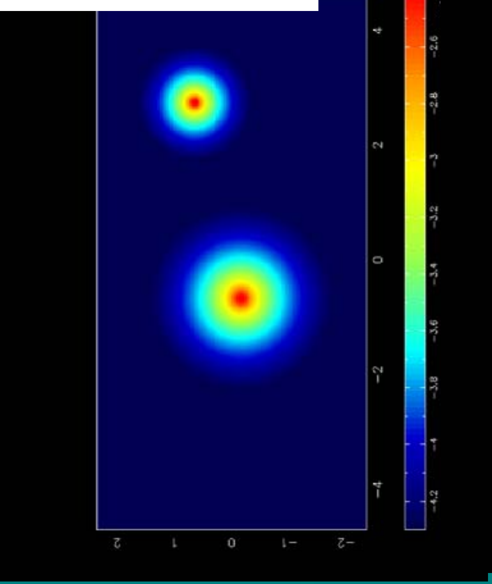

Gas temperature

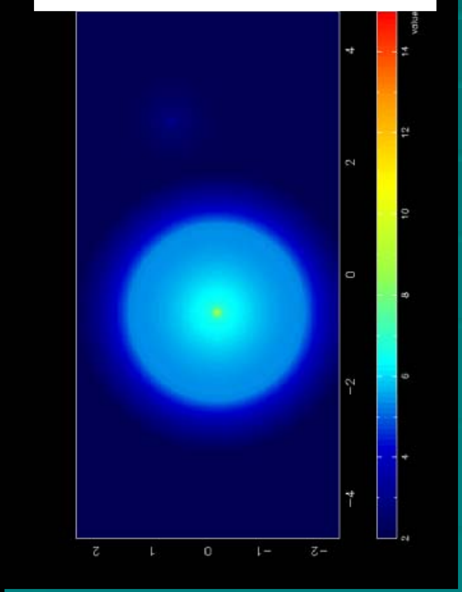

Mass Estimation Method

- Clusters in the simulations are “observed” from certain directions.
- N_{samp}(=100) particles are randomly selected, and recognized as “galaxies whose line-of-sight velocity are observed”.
- Virial mass is calculated as follows.

$$M_{\rm VT} = \frac{3\pi}{G}\sigma_{\rm los}^2 \left\langle \frac{1}{r} \right\rangle^{-1}$$

$$\left\langle \frac{1}{r} \right\rangle^{-1} = N_p \left(\sum_{i>j}^{N_p} \frac{1}{r_{ij}} \right)$$

r_{ij}: distance projected on the sky plain for particle pairs
σ_{los}:dispersion of line-of-sight velocity

- X-ray surface brightness profile *Ix(R)* and spectroscopic-like temperature profile *T(R)* are made from the simulation data.
- Density profiles $\rho(r)$ are calculated from *Ix(R)* with a standard deprojection technique.
- Both $\rho(r)$ and *T(r)* are fitted with β -model.
- Assuming hydrostatic equilibrium, the mass profiles are calculated as follows,

$$M_r = -\frac{k_{\rm B} T_{\rm g} r}{G\mu m_{\rm p}} \left(\frac{d\ln\rho_{\rm g}}{d\ln r} + \frac{d\ln T_{\rm g}}{d\ln r} \right)$$

Mass estimation during core passage

X-ray data seen along the collision axis

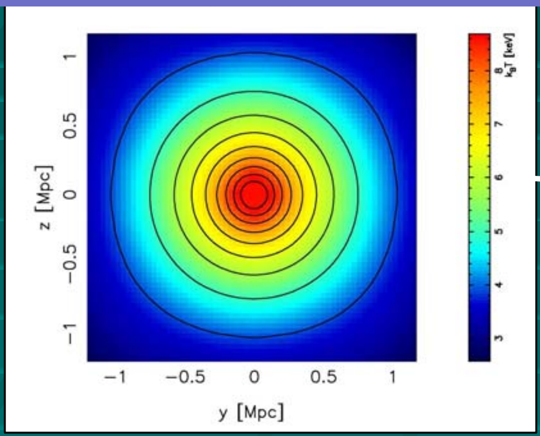

solid lines : M_{real}
dashed lines : M_X
asterisks : M_{virial}

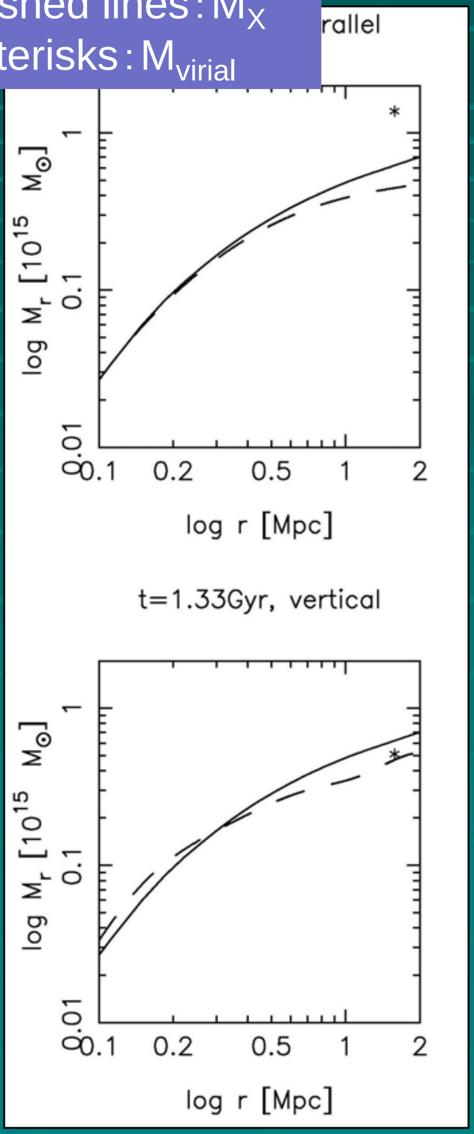

solid lines : M_X /M_{real}
asterisks : M_{virial} /M_{real}

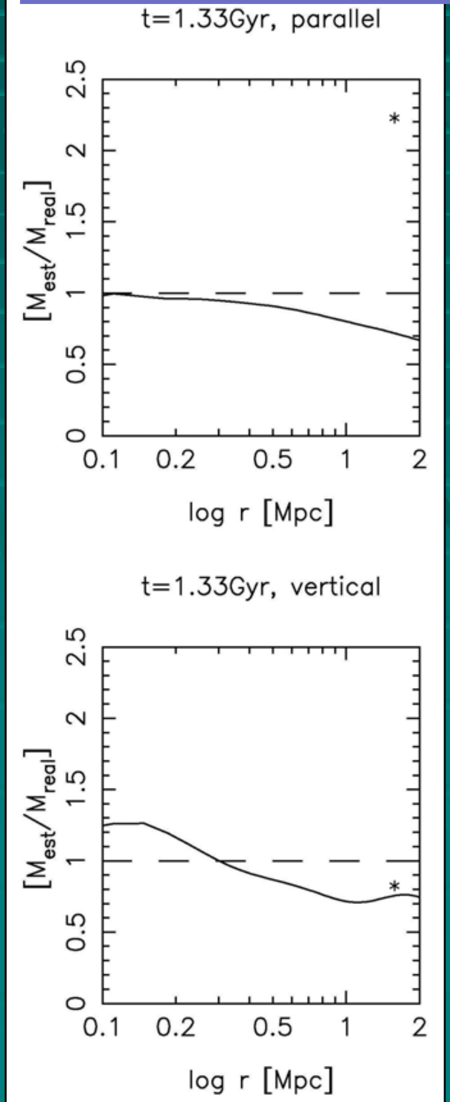

X-ray data seen from the direction perpendicular to the collision axis

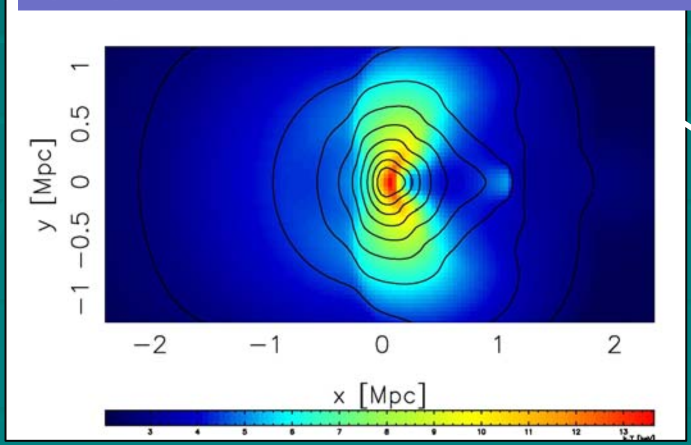

Mass estimation after core passage

X-ray data seen along the collision axis

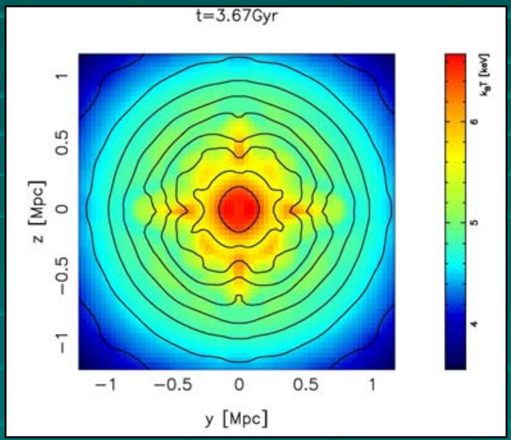

X-ray data seen from the direction perpendicular to the collision axis

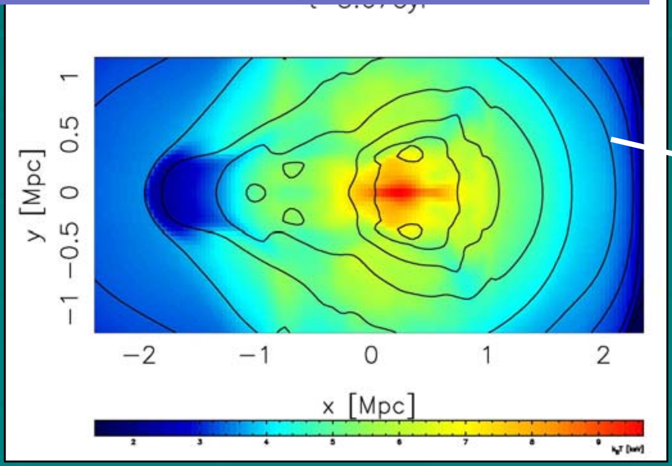

solid lines： M_{real}
Dashed lines：M_X
asterisks：M_{virial}

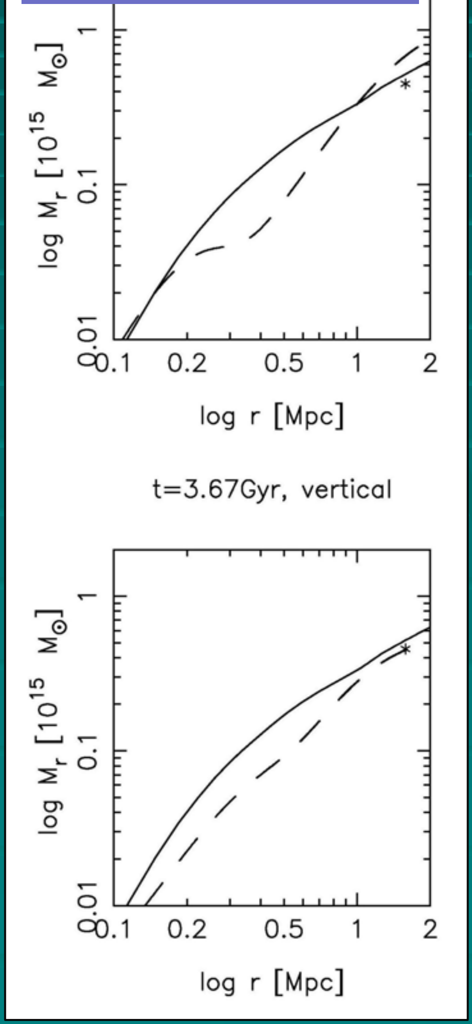

solid lines： M_X /M_{real}
asterisks： M_{virial} /M_{real}

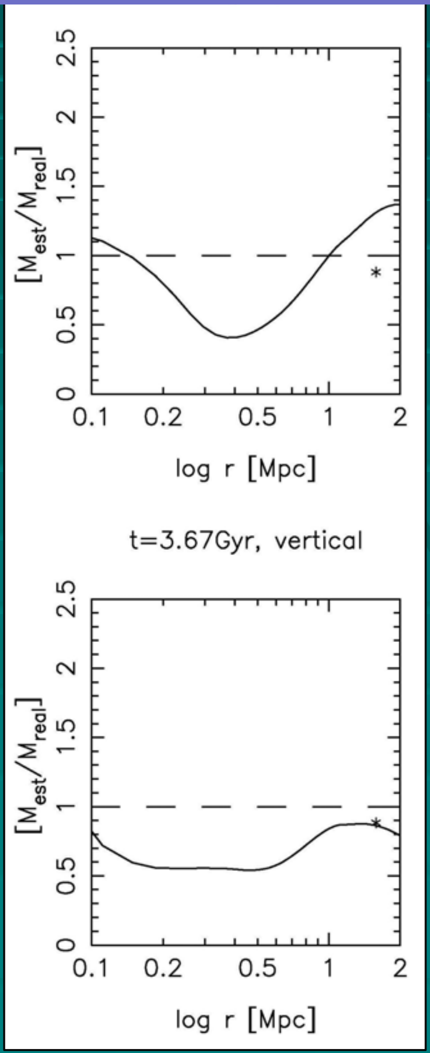

Surface mass density (comparison with “lensing results”)

Lensing potential depends on the surface mass density.
「M_{prj}(R) mass within a cylinder」 is more direct results than 「M(r) mass within a sphere」

M(r) derived from X-ray data are converted into M_{prj}(R), which are compared with “real projected mass”.

$$M_{\rm prj}(R) = \int_0^R 2\pi R' \Sigma(R') dR',$$

$$\Sigma(R) = 2\int_0^{b_{\rm out}} \rho(\sqrt{R^2+b^2}) db,$$

$$\rho(r) = \frac{1}{4\pi r^2}\frac{dM}{dr}.$$

Mimic of comparison with gravitational lensing data

Projected Mass Results (Comparison with "lensing Results")

During core passage

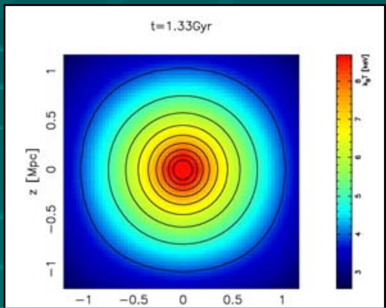

Seen from the direction along the collision axis

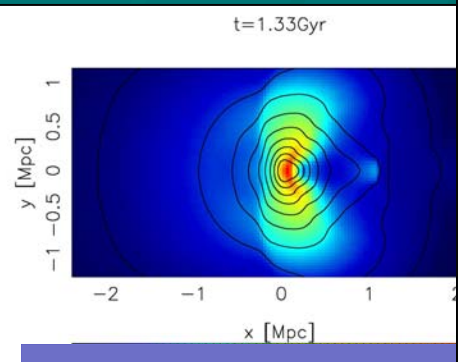

Seen from the direction perpendicular to the axis

Solid lines : M_{real}
Dashed lines : M_X asterisks : M_{virial}

Solid lines : M_X/M_{real}
Dotted lines : 1 asterisks : M_{virial}/M_{real}

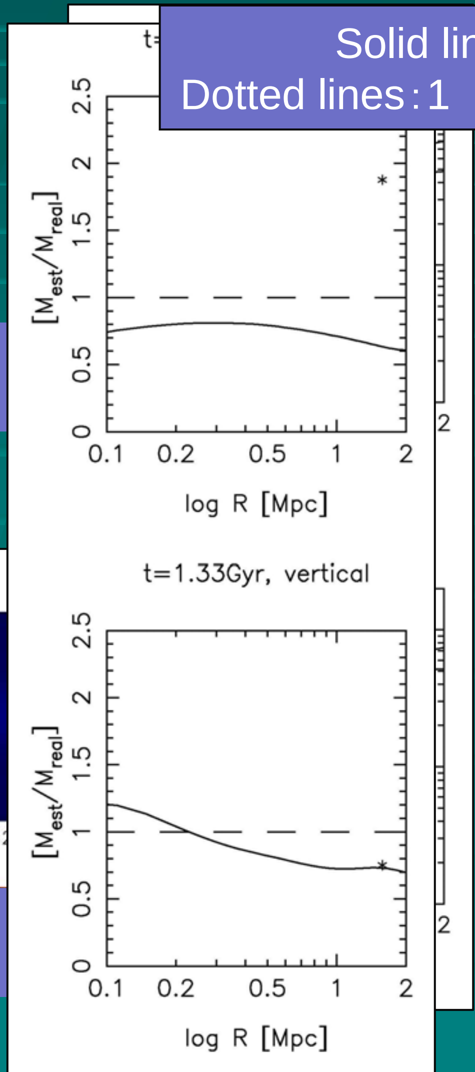

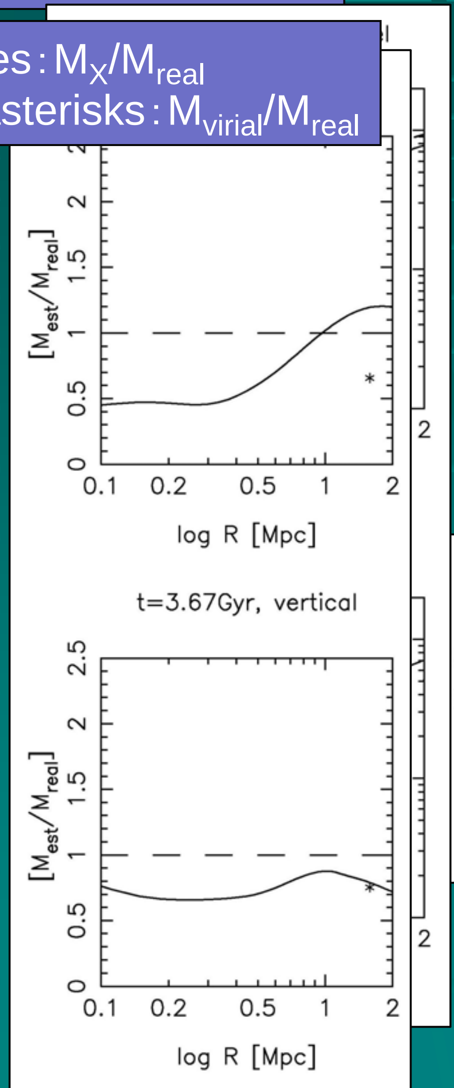

After core passage

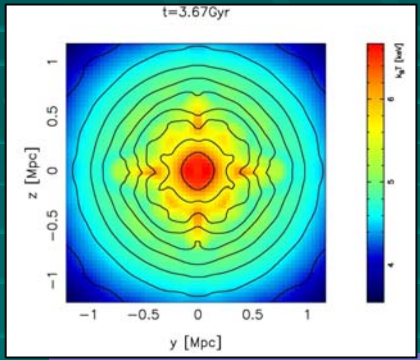

Seen from the direction along the collision axis

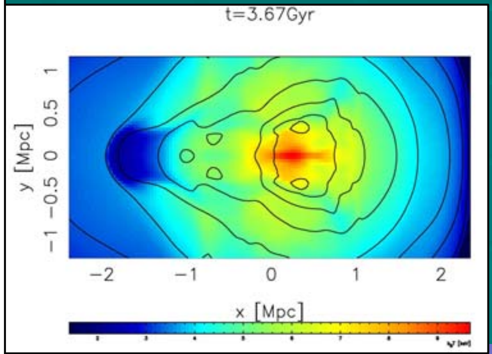

Seen from the direction perpendicular to the axis

X-ray morphology and mass estimation uncertainity

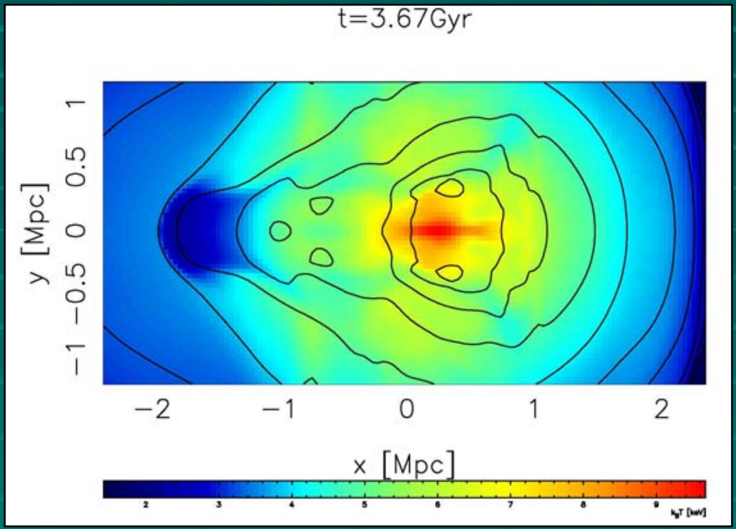

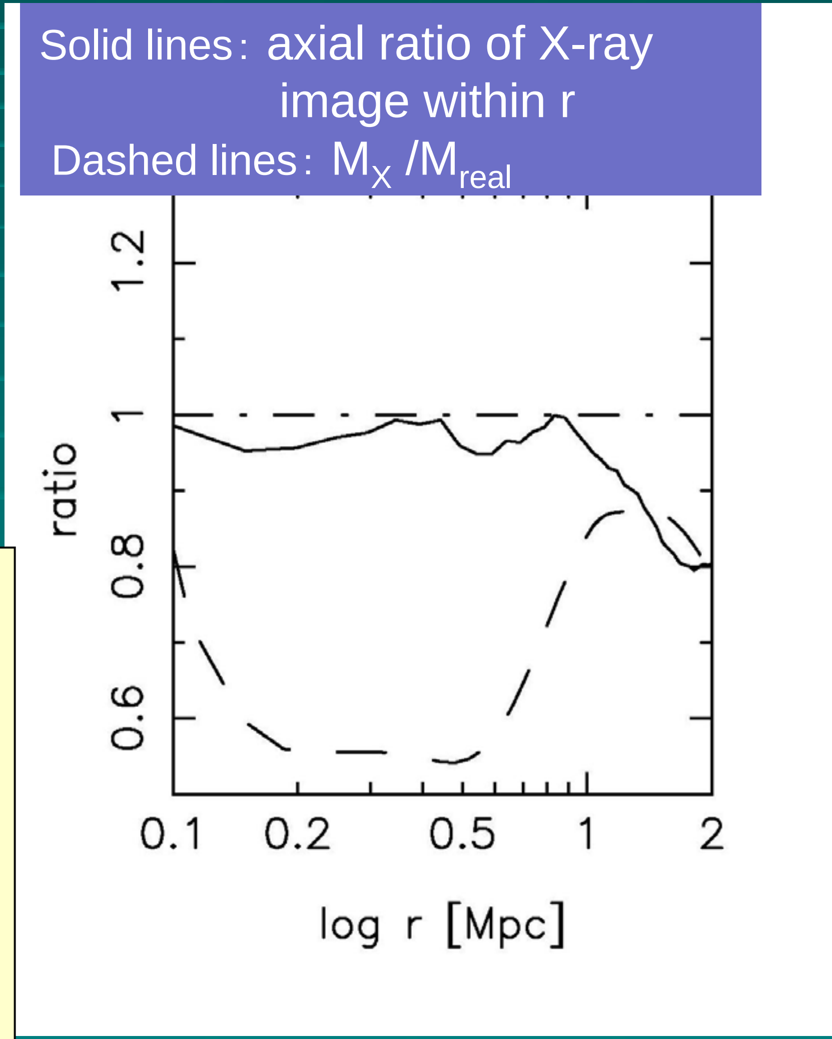

•Morpholgy depends on the radius within which it is estimated.
•This cluster looks “round” only in the inner part, but its mass is underestimated by over 40 %.

If this cluster is located at high redshift and hence only the inner part can be observed, what happens?

Summary

- We investigate the impact of mergers on the mass estimation of galaxy clusters using simulation data.
- The dependence of observational directions is weaker in case of mass estimation with X-ray data than virial mass estimation
- When the system is observed along the collision axis, the projected mass tends to be underestimated, which should be noted when virial and/or X-ray mass is compared with gravitational lensing results.
- X-ray morphology determined from only the inner region is not a good indicator of mass estimation error, which should be cared for distant faint clusters.
- Takizawa et al. 2010 PASJ, 62, 951